**SUPPLEMENTARY METHODS and MATERIALS FOR Biallelic variants in *SLC4A10* encoding the sodium-dependent chloride-bicarbonate exchanger NCBE lead to neurodevelopmental disorder.**

**SUPPLEMENTARY METHODS**

**Supplementary Methods 1. Splicing Assay**

**SUPPLEMENTARY RESULTS**

**SUPPLEMENTARY FIGURES**

**Supplementary Figure 1 Phasing of the variants identified in family 2.**

**Supplementary Figure 2 Genome-wide homozygosity mapping from ES data.**

**Supplementary Figure 3 Multiple sequence alignment.**

**Supplementary Figure 4 The *SLC4A10* c.81+2T>C variant causes exon skipping.**

**Supplementary Figure 5 Expression of alternatively spliced transcripts of *SLC4A10.***

**Supplementary Figure 6 Neuroimaging features.**

**SUPPLEMENTARY TABLES**

**Supplementary Table 1 List of Primer Sequences**

**Supplementary Table 2 Table of characteristics of *SLC4A10* variants**

**Supplementary Table 3 Table of additional unknown significance variants identified in sequencing data from the patients**

**Supplementary Table 4 *In silico* splice prediction scores**

**Supplementary Table 5 Extended clinical details**

**Supplementary Table 6 Table of Detailed facial dysmorphic features**

**Supplementary Table 7 Table of the frequency of each dysmorphic feature in the patients**

**SUPPLEMENTARY METHODS:**

**Supplementary Methods 1. Splicing Assay**

A region spanning part of SLC4A10 intron 1 (343 bp) and intron 2 (259 bp), containing the complete 5´ UTR (55 bp) and Exon 2 (81 coding bp) sequences was directly PCR-amplified from patient (mutant) and wild-type genomic DNA samples with primers containing additional XhoI and BamHI restriction sites listed in Supplementary Table 1. Clean-up and restriction enzyme digestion of the PCR amplicon and pSPL3 exon trapping vector was performed prior to ligation between the vector-containing exons A and B of the linearized vector. The vector was transformed into DH5α competent cells (NEB 5-alpha, New England Biolabs, Frankfurt, Germany), plated and incubated overnight. Colonies with patient and wild-type containing sequences were selected for correct size using colony PCR with an SD6 forward and the SLC4A10-specific reverse primer. Colonies with an insert of the correct size were used to inoculate overnight cultures of liquid LB-ampicillin for plasmid isolation. The wild-type and mutant-containing vector sequences were confirmed by Sanger sequencing.

A limitation of the minigene assay is that splicing machinery cannot recognize the splice acceptor-deficient first coding exon. To facilitate recognition of exon 2, we used site-directed mutagenesis (SDM) at position c.-8G>T to create a "decoy" splice acceptor site at position c.-3. (NEB Q5 Site Directed Mutagenesis Kit, New England Biolabs, Frankfurt, Germany) per manufacturer's protocol. SDM primers were designed with NEBase Changer version 1.3.3 (New England Biolabs, https://nebasechanger.neb.com/). Colonies cultured overnight for next-day plasmids isolation were Sanger sequence verified.

The sequence-confirmed vectors with mutant and wild-type sequence, as well as two replicates each of the SDM-treated plasmids were transfected into HEK 293T cells (ATCC, Manassas, VA, USA) as previously described (1). RT-PCR followed using vector-specific SD6 forward and SA2 reverse primers. Initial sequencing of the SDM-wild-type (c.81+2T) cDNA showed double peaks, prompting TA cloning with the pCR2.1 vector (ThermoFisher, Darmstadt, Germany) following standard protocols. Colonies cultured overnight for next-day plasmid extraction were Sanger sequence-verified using M13 primers. The amplified fragments were visualized on a 1% agarose gel and Sanger sequenced.

**SUPPLEMENTARY RESULTS**

**Dysmorphological assessment**

Facial photographs and videos reviewed for 7 children from 3 families (Patients 4-10 from Families 3, 4 and 5). No photographs were available for review from patients 1-3 from Families 1 and 2). Figure 4A shows the facial photographs of all 7 patients. Their dysmorphic features were described based on terminology recommended by Elements of Morphology. Where no term was available for a dysmorphic feature seen in a patient, HPO terminology was used instead. Detailed facial dysmorphic

features for all 7 patients are shown in Table 1 and they are tabulated using unique HPO IDs in Supplementary Table 7 to generate frequency of each feature.

**SUPPLEMENTARY FIGURES**

**Supplementary Figure 1. Phasing details of 2 missense variants identified in patient 3 from Family 2**

**A.** Genomic DNA samples from F2:I1 and F2:II1 were emulsified into aqueous droplets in an oil-aqueous reverse emulsion. Allele-specific fluorescence probes were used to detect alleles at two different loci (GRCh38; chr2:161905754 C>T, c.1864C>T (p.Arg622Trp)-FAM, blue; and GRCh38; chr2:161879234 G>C, c.1052G>C (p.Arg351Thr)-HEX, green). Depending on the alleles in the droplets, they would be positive for one fluorophore (blue or green), positive for both fluorophores (orange), or positive for neither fluorophore after PCR. Trans-alleles partition into droplets independently. Therefore, co-partitioning (orange) is determined by chance. Cis- alleles tend to co-segregate into the same droplets; co-partitioning significantly exceeds random expectations. **B.** Co-partitioning of the two alleles could be disrupted by restriction enzyme digestion at a site between the cis-alleles; then co-partitioning would happen to the amount predicted by chance. RsaI restriction enzyme was used and droplet populations are the same before and after digestion. As a result, variants seem to have a trans configuration (2).

**Supplementary Figure 2 Genome-wide homozygosity mapping from WES data.**

The AutoMap tool (3) was used to create homozygosity mapping for the 4 probands harbouring homozygous *SLC4A10* variant (F1:IV5, F3:V4, F4:V2, and F5:V8). The identified SLC4A10 variant-containing regions of homozygosity are shown in the red rectangle. (Blue regions represent detected ROHs.)

**Supplementary Figure 3 Multiple sequence alignment.**

Multi-species alignments of SLC4A10, showing locations of the conserved residues (asterisk) and each of the missense variants identified in this study (in black rectangle).

**Supplementary Figure 4 The SLC4A10 c.81+2T>C variant causes exon skipping. A.** Schematic illustration of the minigene constructs and RT-PCR results for the c.81+2T>C variant. The pSPL3 vector contains two exons (exons A and B, purple) spanning a multiple cloning site with *Xho*I and *Bam*HI restriction sites that were used for cloning of the intron 1 (343 bp) and intron 2 (259 bp)-spanning region that include the 5´ UTR (grey, 55 bp) and exon 2 (81 bp, ATG start codon marked in green) regions (light blue). The c.-8G>T variant that was created through site-directed mutagenesis (SDM) is indicated by an upward pointing arrow. Gel electrophoresis of the reverse-transcription polymerase chain reaction (RT-PCR) from the variant (c.81+2C), wild-type (WT, c.81+2T), and empty pSPL3 vector amplicons, as well as transfection-negative control shown to the right. Sanger sequencing confirmed the identity of the normally spliced and exon 2-skipping amplicons, that are equivalent to the empty vector control. **B.** In silico splice predictions of the wild-type (top, red T) and c.81+2T>C (bottom, red C) show near-unanimous abolishment of the native splice donor site. **C.** In silico splice predictions of the modified (c.-8G>T) 5´ UTR of *SLC4A10* by SDM show the creation of an artificial splice acceptor site

at position c.-3 to allow exon-recognition and thus provide an RNA-level assay read-out. **D.** The SDM modification at position c.-8 is necessary for 5´ UTR and exon 2-inclusion in the WT construct and allows assessment of the c.81+2T>C canonical splice variant. The gel electrophoresis shows RT-PCRs of non-SDM treated (lanes 2 and 5) versus SDM-treated (lanes 3-4 and 6-7) pSPL3 constructs containing the c.81+2C variant and WT (c.81+2T) amplicons, respectively. Each variant and WT transfection using plasmids subjected to SDM were performed twice. Lane 1: 100 bp ladder, Lane 2: pSPL3 *SLC4A10* c.81+2C variant SDM negative, Lane 3; pSPL3 *SLC4A10* c.81+2C variant replicate 1, Lane 4: pSPL3 *SLC4A10* c.81+2C variant replicate 2, Lane 5: pSPL3 *SLC4A10* c.81+2T WT SDM negative, Lane 6: pSPL3 *SLC4A10* c.81+2T WT replicate 1, Lane 7: pSPL3 *SLC4A10* c.81+2T WT replicate 2, Lane 8: PCR negative control. White arrows indicate faint bands.

**Supplementary Figure 5 Expression of alternatively spliced transcripts of *SLC4A10***

The *SLC4A10* MANE select transcript used for annotating variants is NM_001178015.2/ENST00000446997.6 (black arrow) while the transcript that was used for testing the c.81+2T>C variant corresponds to NM_001178016.1/ENST00000375514.9 (blue arrow), ranked second and third in terms of isoform expression, respectively. Exon 2 harbouring the c.81+2T>C variant is boxed in black. Source: https://gtexportal.org/home/gene/SLC4A10

**Supplementary Figure 6 Neuroimaging features.**

Gray matter nodular heterotopias in three subjects with SLC4A10 variants (P1, P2 and P3). Axial (A, E, I) and sagittal (B, C, F, G, J, K) reformatted 3D T1 weighted images and coronal T2-weighted (D, H, L) images demonstrate multiple small nodules of gray matter heterotopia extending from the temporo-occipital periventricular regions to the temporo-occipital cortex with a peculiar curvilinear disposition (yellow arrows).

**SUPPLEMENTARY TABLES**

**Supplementary Table 1 List of Primer Sequences**

| Minigene assay | |
|---|---|
| hu SLC4A10 Ex2 XhoI F | aattctcgagTTTGCAACAGACACATTGGA |
| hu SLC4A10 Ex2 BamHI R | attggatccCTCTTCCTTTACCGCCCTCT |
| Site-directed mutagenesis | |
| Q5SDM_SLC4A10_c.-8G_T_F | TCTTTTGTAAtACAGGAAATGCAG |
| Q5SDM_SLC4A10_c.-8G_T_R | TAATCACAGCCATCTCTATG |
| Sequencing | |
| SD6 F | TCTGAGTCACCTGGACAACC |
| SA2 R | ATCTCAGTGGTATTTGTGAGC |
| M13 F | GTAAAACGACGGCCAG |
| M13 R | CAGGAAACAGCTATGACC |

All sequences are given in the 5' to 3' direction.

**Supplementary Table 2. Variant Table**

*Available as a separate excel file*

**Supplementary Table 3 Variants identified in WGS-WES**

*Available as a separate excel file*

**Supplementary Table 4 In silico splice prediction scores**

| | Splice-site Finder [0-100] | | | MaxEnt [0-12] | | | NNSPLICE [0-1] | | | GeneSplicer [0-24] | | |
|---|---|---|---|---|---|---|---|---|---|---|---|---|
| | Wild-type | Mutant | % change | Wild-type | Mutant | % change | Wild-type | Mutant | % change | Wild-type | Mutant | % change |
| c.81 splice donor[1] | 84.50 | 81.70 | -3.3% | 9.46 | 0 | -100% | 0.99 | 0 | -100% | 1.61 | 0 | -100% |
| c.-3 decoy splice acceptor[2] | 0 | 91.17 | +91.17 % | 0.79 | 6.30 | 697.8% | 0 | 0.67 | +67% | 0 | 3.81 | +15.9% |

[1]Change in splice prediction scores at the native c.81 splice donor site due to the c.81+2T>C variant.

[2]Site-directed mutagenesis of a c.-8G>T variant created a new splice acceptor site at the c.-3 position.

**Supplementary Table 5 Extended clinical table.**

*Available as a separate excel file*

**Supplementary Table 6 Detailed facial dysmorphic features.**

*Available as a separate excel file*

**Supplementary Table 7 The frequency of each dysmorphic feature.**

*Available as a separate excel file*

**Table of clinical details of patient 11 from family 6**

| |
|---|
| **Seizures: yes** |

**seizure type:**

1.) Epileptic spasms
2.) Dialeptic seizures
3.) Myoclonic seizures
4.) Atonic seizures

**Frequency of seizures before and after therapy (intractable seizures/seizure controlled with [please specify medication])**

Intractable seizures with a frequency of several seizures per hour

**Duration: minutes**

**Age of onset: first year of life**

**evolution**

**Status epilepticus**
**never**

**Clustering**
**no**

**Associated manifestations:**

Profound global developmental delay
Dystonic movement disorder
Muscular hyptonia
Feeding difficulties (PEG feeding)
Bilateral hip luxation

**EEG (Initial and follow up)**

1. Dialeptic and myoclonic seizures
2. Spikes and spike-wave complexes bilaterally
3. Continuous slowing bifrontal

**Anti-epileptic drugs (AEDs) (indicate drug, duration of therapy and response to therapy)**

Previous drugs without response to therapy
Sultiame (12.08.2014 – 13.01.2015)
Clobazame (01.09.2014 – 06.03.2015)
Vigabatrine (02.09.2014 – 23.04.2015)
Vitamin B6 (20.12.2014 – 20.01.2015)
Pulsatile Steroids Methylprednisolonee) in August 2014
Topiramate (23.01.2015 – 10.10.2015)
Ethosuximide (11.06.2015 – 02.07.2015)
Valproate (07.08.2015 – 18.10.2015)
Levetiracetam (25.01.2016 – 04.02.2016)
Modified Atkins diet (14.10.2015 – 15.04.2016)
Dronabinol (09.03.2016 – 28.08.2016)
Lacosamide 2018
Perampanel (05.06.2018 – August 2018)
Oxcarbazepin (24.08.2021 – 24.09.2021)
Lamotrigin März 2022
Cannabidiol 11/2021 – 01/2022
Current treatment: Dronabinol

## Clinical delineation of patient 11 from family 6

The 9-year-old affected girl from family 6 was suffered from seizures starting in the first year of life, which were described as infantile spasms, myoclonic, dialeptic and atonic seizures (further clinical details in the supplementary material). Seizures were intractable with a frequency of several seizure attacks per hour that last a few minutes. She has a severe-to-profound GDD/ID, muscular hypotonia, and progressive choreiform and dystonic movement disorder with feeding difficulties (PEG feeding) and bilateral hip luxation. Brain MRI at the age of 8 revealed non-specific findings such as the incomplete rotation of the hippocampi and thinning of the corpus callosum.

**Supplementary literature**


1. Tompson SW, Young TL. Assaying the Effects of Splice Site Variants by Exon Trapping in a Mammalian Cell Line. Bio Protoc. 2017;7(10).
2. Regan JF, Kamitaki N, Legler T, Cooper S, Klitgord N, Karlin-Neumann G, et al. A rapid molecular approach for chromosomal phasing. PLoS One. 2015;10(3):e0118270.
3. Quinodoz M, Peter VG, Bedoni N, Royer Bertrand B, Cisarova K, Salmaninejad A, et al. AutoMap is a high performance homozygosity mapping tool using next-generation sequencing data. Nat Commun. 2021;12(1):518.

A

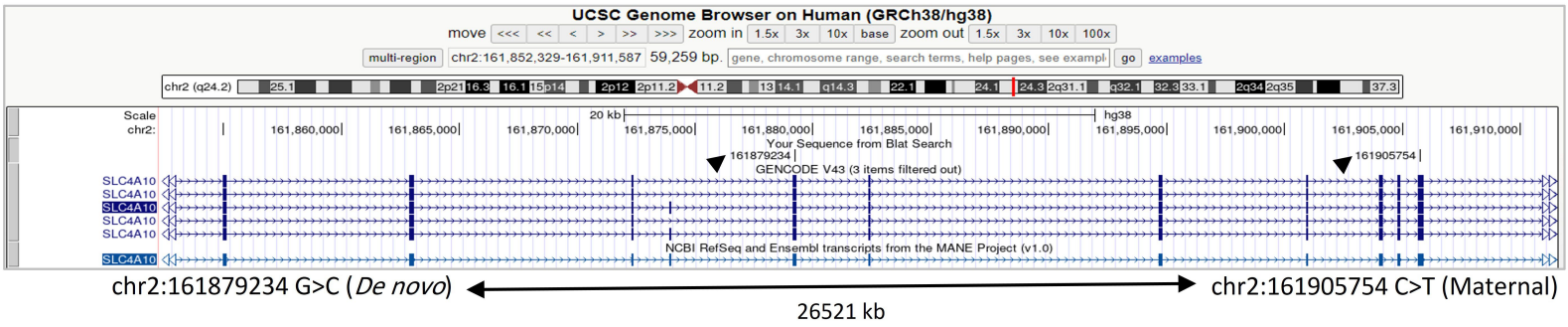


chr2:161879234 G>C (*De novo*) ⟷ chr2:161905754 C>T (Maternal)

26521 kb

Chr2(GRCh38): g.161905754C>T FAM Labeled

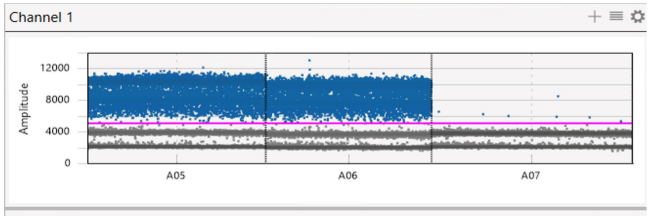


Chr2(GRCh38): g.161879234G>C HEX Labeled

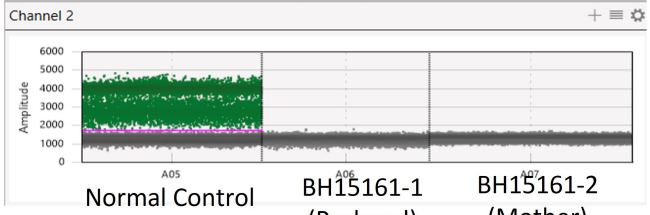


Normal Control | BH15161-1 (Proband) | BH15161-2 (Mother)

BH15161-1 (Proband)

Positive for Mutation 1
Negative for Mutation 2

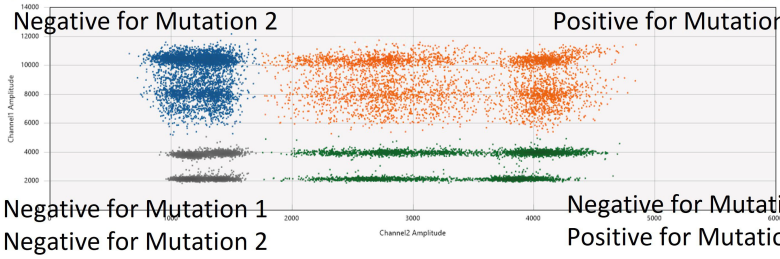


Positive for Mutation 1
Positive for Mutation 2

Negative for Mutation 1
Negative for Mutation 2

Negative for Mutation 1
Positive for Mutation 2

BH15161-2 (Mother)

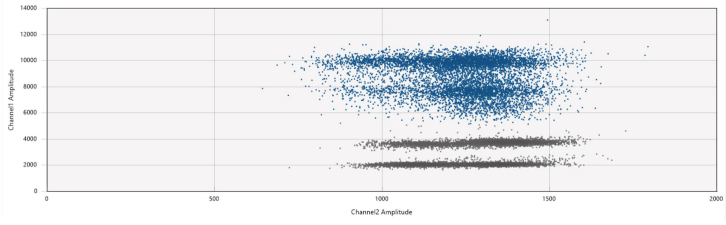


BH15161-1 (Proband)

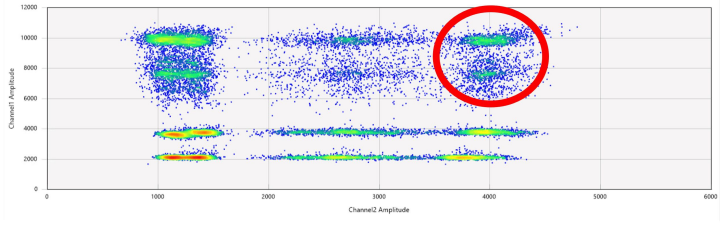


B

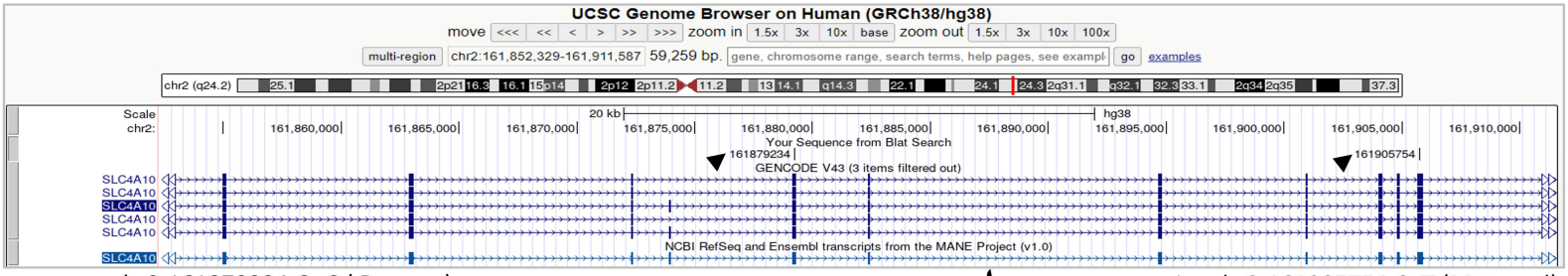


chr2:161879234 G>C (*De novo*) ⟷ chr2:161905754 C>T (Maternal)

26521 kb

*RsaI*

BH15161-1 (Proband) Digestion with *RsaI* No RS Digestion

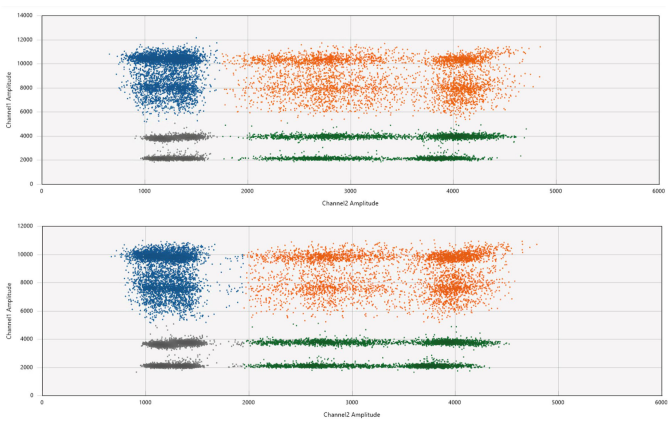


| Ch1+Ch2+ | Ch1+Ch2- | Ch1-Ch2+ | Ch1-Ch2- |
|---|---|---|---|
| 4425 | 4677 | 4623 | 4733 |
| 4425 | 4677 | 4623 | 4733 |

| Ch1+Ch2+ | Ch1+Ch2- | Ch1-Ch2+ | Ch1-Ch2- |
|---|---|---|---|
| 4498 | 4792 | 4886 | 4973 |
| 4498 | 4792 | 4886 | 4973 |

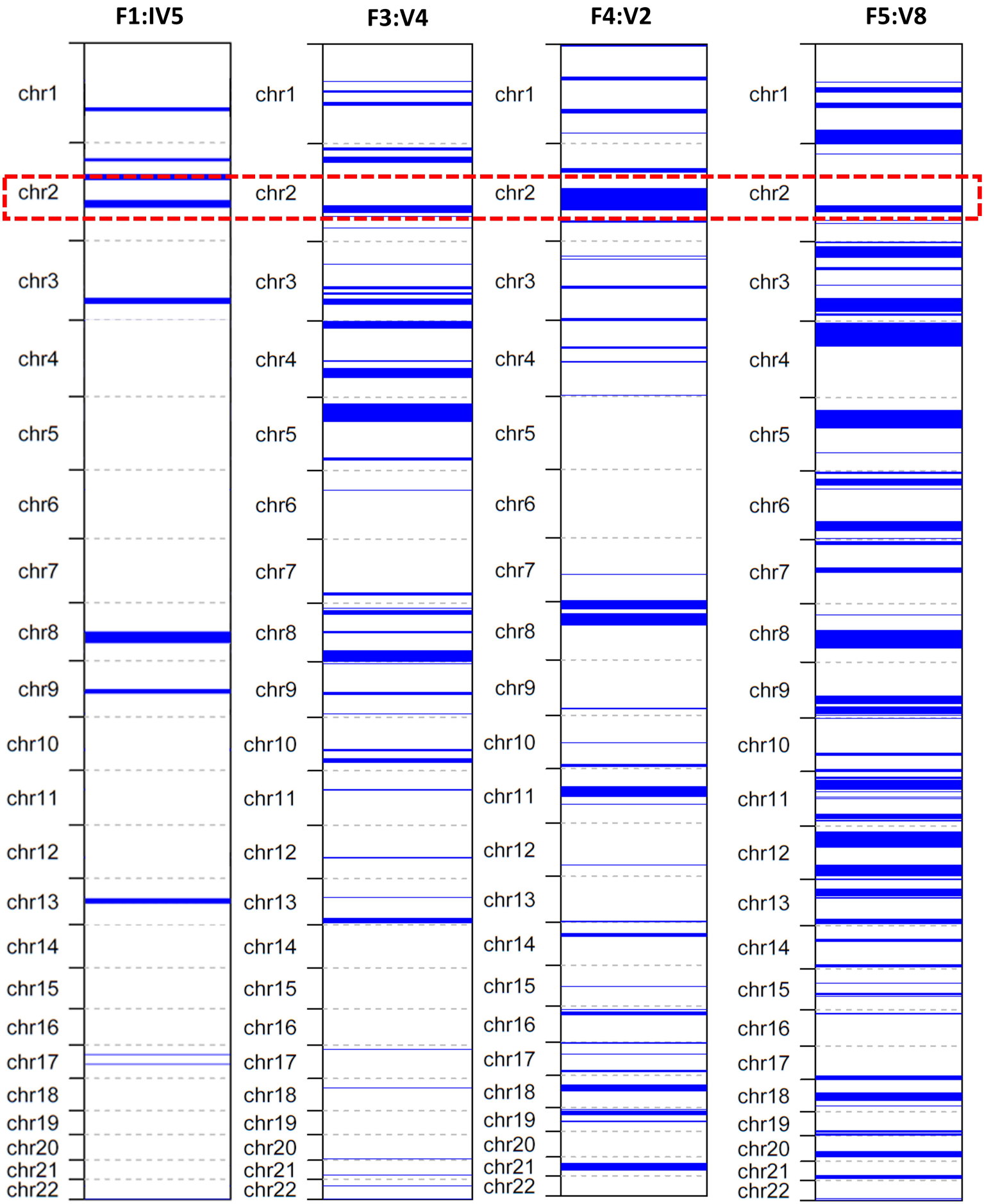
F1:IV5
F3:V4
F4:V2
F5:V8
chr1
chr2
chr3
chr4
chr5
chr6
chr7
chr8
chr9
chr10
chr11
chr12
chr13
chr14
chr15
chr16
chr17
chr18
chr19
chr20
chr21
chr22

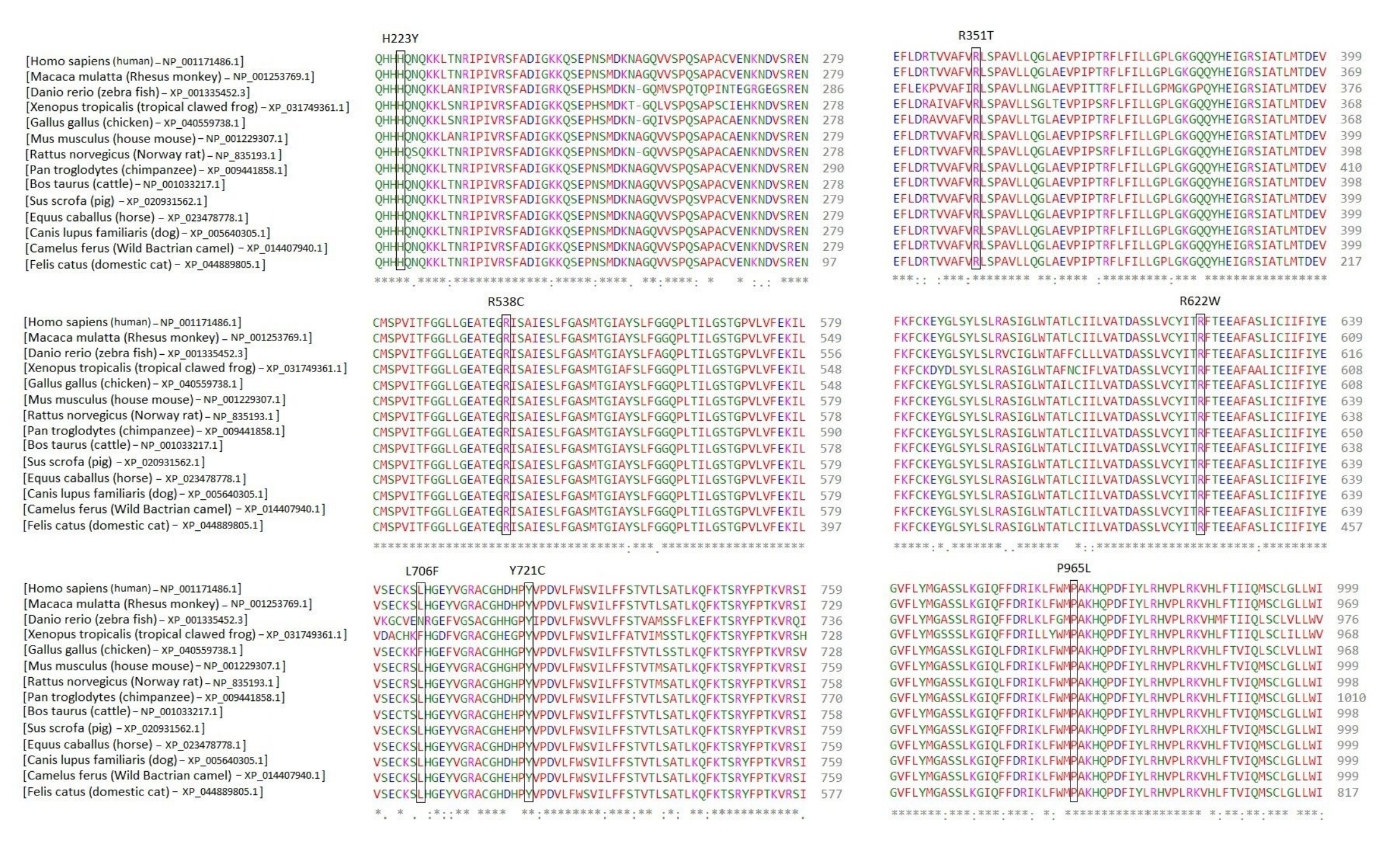
H223Y
R351T
[Homo sapiens (human) – NP_001171486.1]
[Macaca mulatta (Rhesus monkey) – NP_001253769.1]
[Danio rerio (zebra fish) – XP_001335452.3]
[Xenopus tropicalis (tropical clawed frog) – XP_031749361.1]
[Gallus gallus (chicken) – XP_040559738.1]
[Mus musculus (house mouse) – NP_001229307.1]
[Rattus norvegicus (Norway rat) – NP_835193.1]
[Pan troglodytes (chimpanzee) – XP_009441858.1]
[Bos taurus (cattle) – NP_001033217.1]
[Sus scrofa (pig) – XP_020931562.1]
[Equus caballus (horse) – XP_023478778.1]
[Canis lupus familiaris (dog) – XP_005640305.1]
[Camelus ferus (Wild Bactrian camel) – XP_014407940.1]
[Felis catus (domestic cat) – XP_044889805.1]
R538C
R622W
L706F
Y721C
P965L

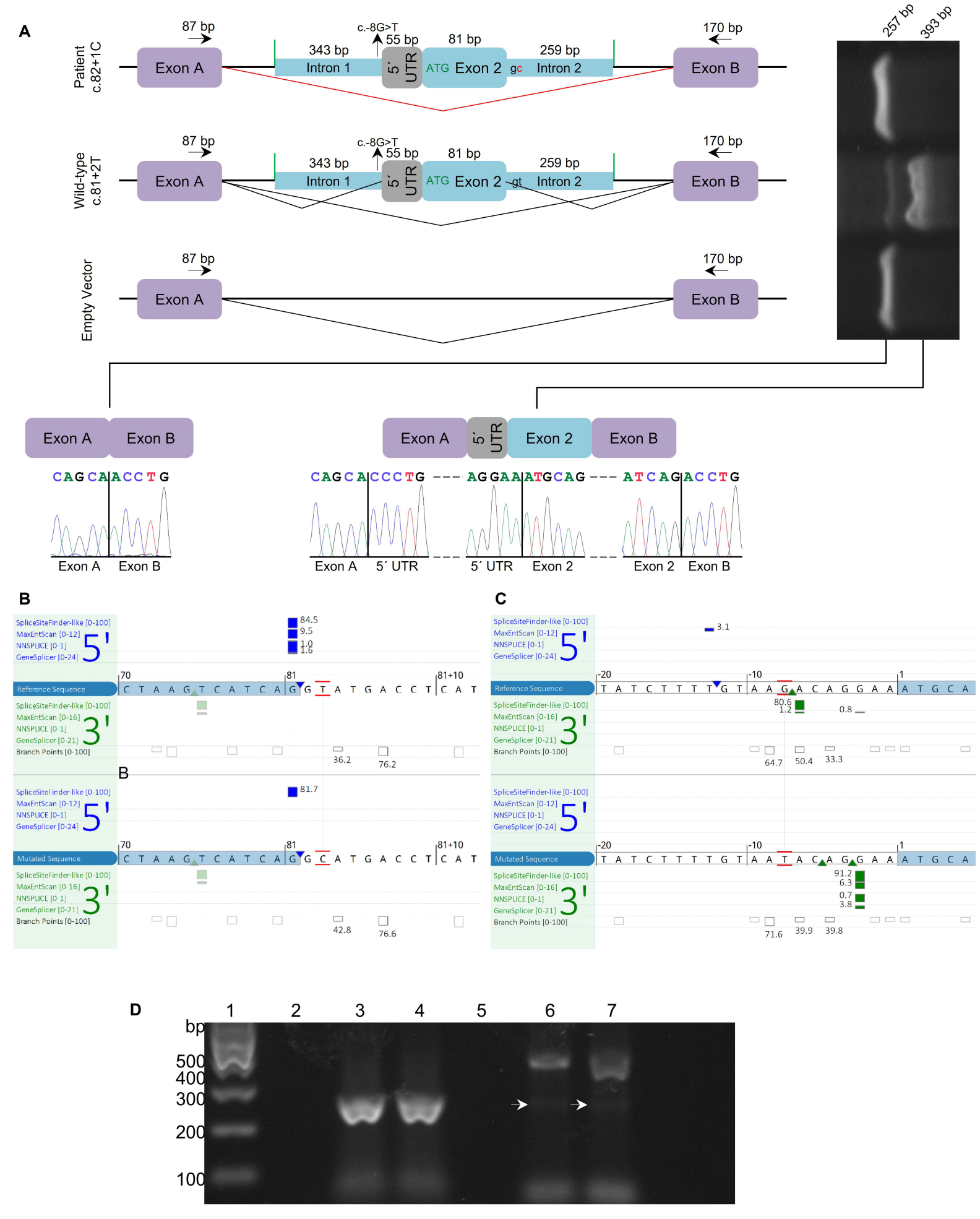
A
Patient c.82+1C
Wild-type c.81+2T
Empty Vector
87 bp
170 bp
Exon A
Exon B
343 bp
Intron 1
c.-8G>T
55 bp
5´ UTR
81 bp
ATG Exon 2
259 bp
Intron 2
gc
gt
257 bp
393 bp
Exon A Exon B
Exon A 5´ UTR Exon 2 Exon B
CAGCAACCTG
CAGCACCCTG --- AGGAAATGCAG --- ATCAGACCTG
Exon A Exon B
Exon A 5´ UTR
5´ UTR Exon 2
Exon 2 Exon B
B
C
SpliceSiteFinder-like [0-100]
MaxEntScan [0-12]
NNSPLICE [0-1]
GeneSplicer [0-24]
5'
Reference Sequence
C T A A G T C A T C A G G T A T G A C C T C A T
70
81
81+10
MaxEntScan [0-16]
NNSPLICE [0-1]
GeneSplicer [0-21]
3'
Branch Points [0-100]
84.5
9.5
1.0
1.6
36.2
76.2
Mutated Sequence
C T A A G T C A T C A G G C A T G A C C T C A T
81.7
42.8
76.6
T A T C T T T T G T A A G A C A G G A A A T G C A
-20
-10
1
80.6
1.2
0.8
64.7
50.4
33.3
T A T C T T T T G T A A T A C A G G A A A T G C A
91.2
6.3
0.7
3.8
71.6
39.9
39.8
D
1 2 3 4 5 6 7
bp
500
400
300
200
100

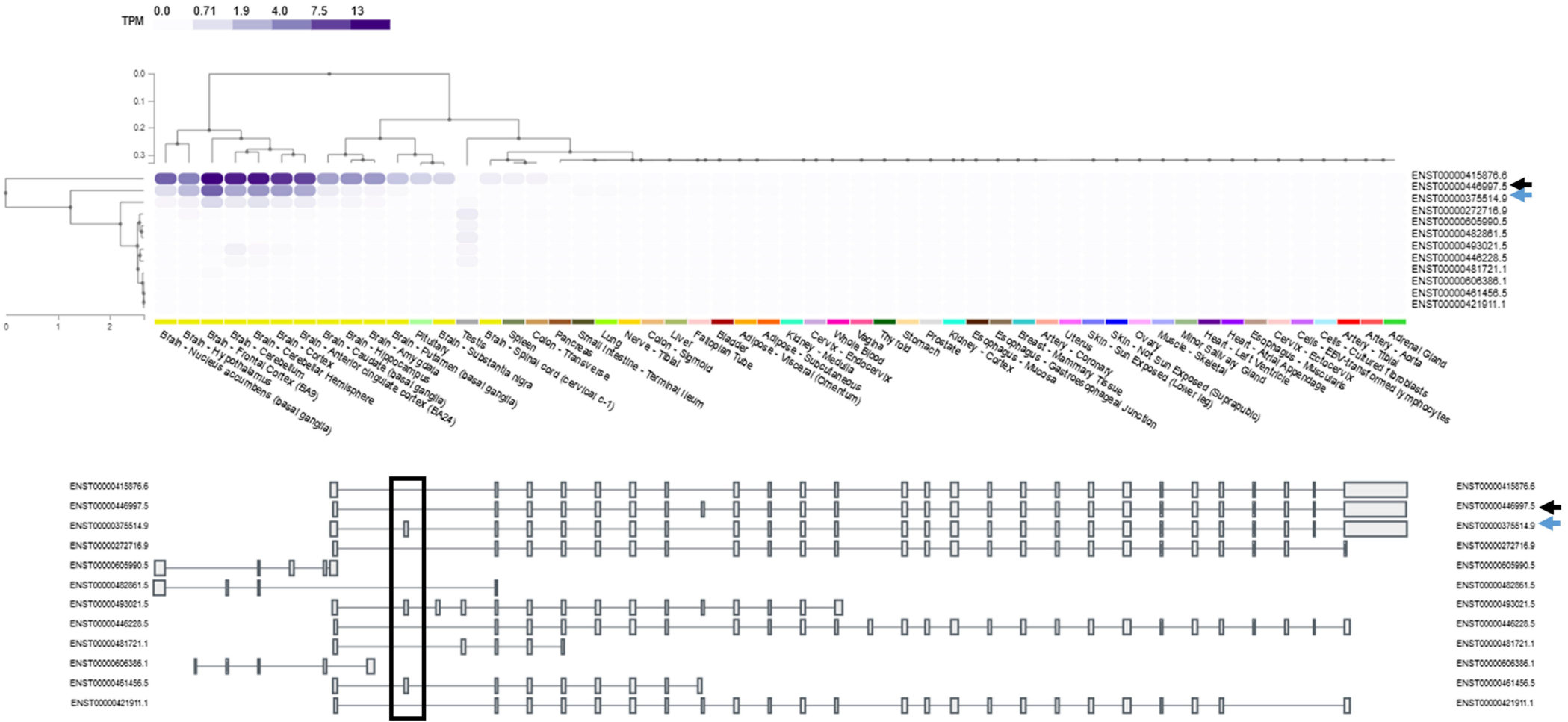
TPM
0.0
0.71
1.9
4.0
7.5
13
ENST00000415876.6
ENST00000446997.5
ENST00000375514.9
ENST00000272716.9
ENST00000605990.5
ENST00000482861.5
ENST00000493021.5
ENST00000446228.5
ENST00000481721.1
ENST00000606386.1
ENST00000461456.5
ENST00000421911.1
Brain - Nucleus accumbens (basal ganglia)
Brain - Hypothalamus
Brain - Frontal Cortex (BA9)
Brain - Cerebellum
Brain - Cerebellar Hemisphere
Brain - Cortex
Brain - Anterior cingulate cortex (BA24)
Brain - Caudate (basal ganglia)
Brain - Hippocampus
Brain - Amygdala
Pituitary
Brain - Putamen (basal ganglia)
Testis
Brain - Substantia nigra
Spleen
Brain - Spinal cord (cervical c-1)
Colon - Transverse
Pancreas
Small Intestine - Terminal Ileum
Lung
Nerve - Tibial
Colon - Sigmoid
Liver
Fallopian Tube
Bladder
Adipose - Subcutaneous
Adipose - Visceral (Omentum)
Kidney - Medulla
Cervix - Endocervix
Whole Blood
Vagina
Thyroid
Stomach
Prostate
Kidney - Cortex
Esophagus - Mucosa
Esophagus - Gastroesophageal Junction
Breast - Mammary Tissue
Artery - Coronary
Uterus
Skin - Sun Exposed (Lower leg)
Skin - Not Sun Exposed (Suprapubic)
Ovary
Muscle - Skeletal
Minor Salivary Gland
Heart - Left Ventricle
Heart - Atrial Appendage
Esophagus - Muscularis
Esophagus - Mucosa
Cervix - Ectocervix
Cells - EBV-transformed lymphocytes
Cells - Cultured fibroblasts
Artery - Tibial
Artery - Aorta
Adrenal Gland

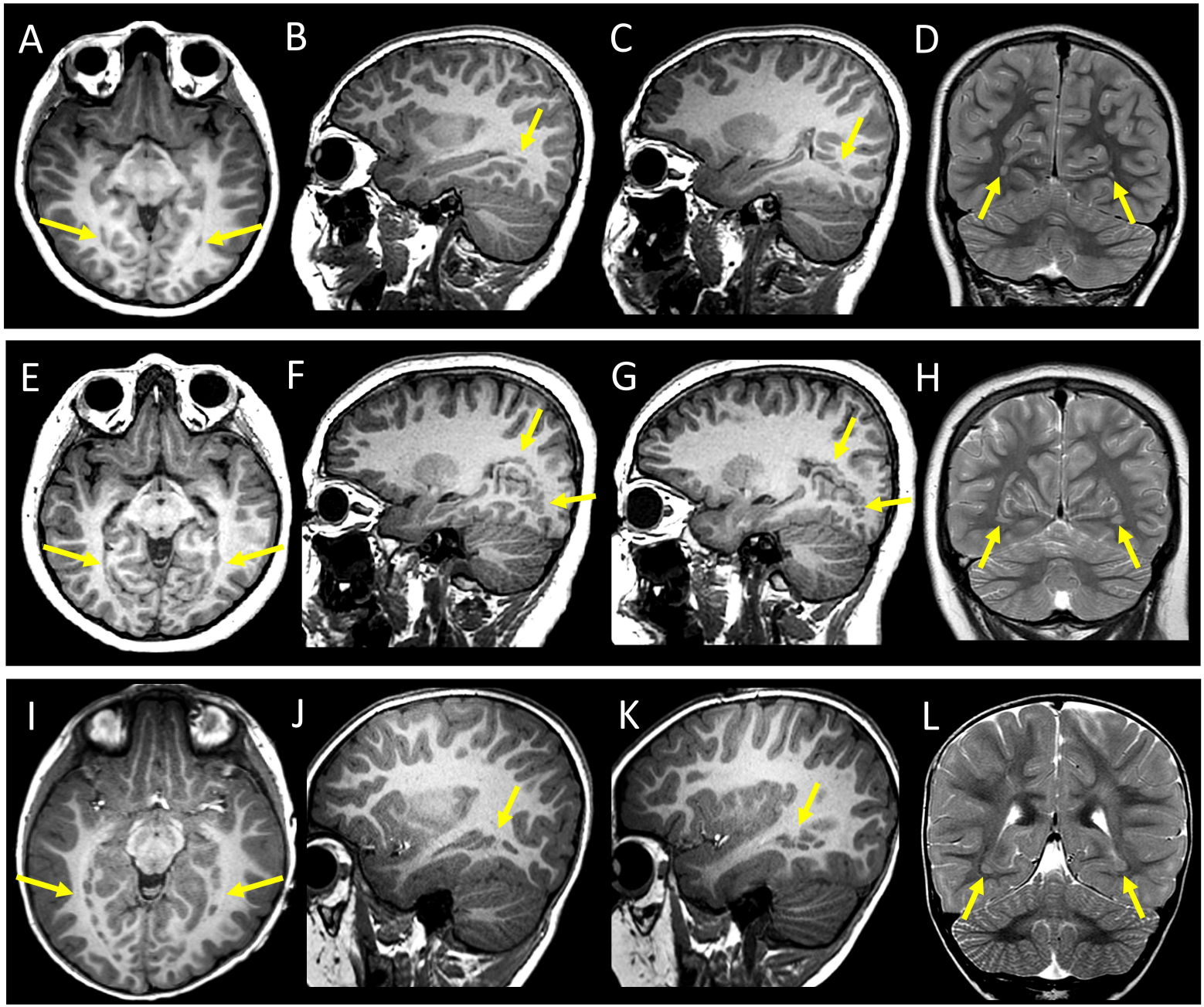
A
B
C
D
E
F
G
H
I
J
K
L